Journal of Orthopaedic Translation 45 (2024) 75–87

Contents lists available at ScienceDirect

Journal of Orthopaedic Translation

journal homepage: www.journals.elsevier.com/journal-of-orthopaedic-translation

Pentamidine-loaded gelatin decreases adhesion formation of flexor tendon

Guidong Shi [a,b], Nakagawa Koichi [b], Rou Wan [b], Yicun Wang [b], Ramona Reisdorf [b], Abigayle Wilson [b], Tony C.T. Huang [c], Peter C. Amadio [b], Alexander Meves [d], Chunfeng Zhao [b,**], Steven L. Moran [c,*]

[a] Department of Orthopaedics, Qilu Hospital of Shandong University, Cheeloo College of Medicine, Shandong University, Jinan, Shandong, China
[b] Department of Orthopedic Surgery, Mayo Clinic, Rochester, MN, USA
[c] Division of Plastic Surgery, Department of Surgery, Mayo Clinic, Rochester, MN, USA
[d] Department of Dermatology, Mayo Clinic, Rochester, MN, USA

ARTICLE INFO

Keywords:
Adhesion
Flexor tendon repair
Gelatin
Pentamidine
Turkey model

ABSTRACT

Background: Prevention of adhesion formation following flexor tendon repair is essential for restoration of normal finger function. Although many medications have been studied in the experimental setting to prevent adhesions, clinical application is limited due to the complexity of application and delivery in clinical translation.
Methods: In this study, optimal dosages of gelatin and pentamidine were validated by gelatin concentration test. Following cell viability, cell migration, live and dead cell, and cell adhesion assay of the Turkey tenocytes, a model of Turkey tendon repair was established to evaluate the effectiveness of the Pentamidine-Gelatin sheet.
Results: Pentamidine carried with gelatin, a Food and drug administration (FDA) approved material for drug delivery, showed good dynamic release, biocompatibility, and degradation. The optimal dose of pentamidine (25ug) was determined in the in vivo study using tenocyte viability, migration, and cell adhesion assays. Further biochemical analyses demonstrated that this positive effect may be due to pentamidine downregulating the Wnt signaling pathway without affecting collagen expression.
Conclusions: We tested a FDA-approved antibiotic, pentamidine, for reducing adhesion formation after flexor tendon repair in both in vitro and in vivo using a novel turkey animal model. Compared with the non-pentamidine treatment group, pentamidine treated turkeys had significantly reduced adhesions and improved digit function after six weeks of tendon healing.
The translational potential of this article: This study for the first time showed that a common clinical drug, pentamidine, has a potential for clinical application to reduce tendon adhesions and improve tendon gliding function without interfering with tendon healing.

1. Introduction

Tendon adhesions are a common clinical problem presenting considerable challenges to the surgeon. Surgical repair of flexor tendon injuries, especially in Zone II area of the hand, are often complicated by adhesions despite improvements in surgical techniques and controlled motion rehabilitation protocols [1]. Designing novel pharmacological or biological therapies to mitigate adhesions remains an unmet clinical need [2–4]. With the development of molecular biology, many cytokines, glycoproteins, and medications have been studied for tendon adhesion prevention, such as TGFβ inhibitors, anti-fibrotic molecules, and lubricin [5–7]. However, food and drug administration (FDA) approved drugs that can directly translate to clinical practice are limited.

Pentamidine (1,5-Bis(4-amidinophenoxy)pentane) is an aromatic diamidine which is pharmacologically utilized as an antiprotazoal agent. It is used in the treatment and prevention of *Pneumocystis carinii* pneumonia (PCP), particularly in patients with HIV infection, and in the treatment of trypanosomiasis and visceral leishmaniasis [8]. Pentamidine has recently been highlighted as a potential anti-cancer drug, particularly in the context of melanoma [9,10]. It has also been demonstrated to have anti-inflammatory properties and data (not published) from our lab has shown that it can inhibit fibrosis in rabbit models of hypertrophic scar. Pentamidine's effects on tendon adhesions

* Corresponding author. Division of Plastic Surgery, Mayo Clinic 200 First Street SW, Rochester, MN, 55905, USA.
** Corresponding author. Department of Orthopedic Surgery, Mayo Clinic, 200 First Street SW, Rochester, MN, 55905, USA.
E-mail addresses: zhaoc@mayo.edu (C. Zhao), Moran.Steven@mayo.edu (S.L. Moran).

https://doi.org/10.1016/j.jot.2023.10.007
Received 13 May 2023; Received in revised form 14 October 2023; Accepted 26 October 2023

have not been evaluated.

Gelatin is a biodegradable material that has been extensively investigated as a drug delivery carrier for many classes of drugs due to its properties as a natural biomaterial and history of safe use in a wide range of medical and pharmaceutical applications. Anti-inflammatory drugs, antineoplastic compounds, antibacterial agents, and recently nucleic acid and hydrophobic materials have been delivered by gelatin, as reported in the literature [11–15]. Drug controlled-release carriers offer many advantages compared to conventional dosage forms, including improved efficacy, maintenance of the desired drug concentration in the blood for a long period of time without reaching a toxic level or dropping below the effective level, reduced toxicity, and improvement in patient compliance and convenience. As a drug delivery carrier, gelatin is versatile due to its intrinsic features that enable the design of different carrier systems [16].

Animal models have been extensively used for flexor tendon repair related research including large animals such as dogs and small animals such as rats. However, in translational research a large animal model is preferred, as the clinically relevant repairs and post-care can be performed. Recently, a novel turkey flexor tendon model was introduced with several advantages compared with other large animal models including large tendon size comparable to human flexor tendon [6], comparable biological responses to injury and healing, sufficient availability, and lack of concerns of using human companion animals such as dogs [17].

The purpose of this study was to investigate the effects of pentamidine delivered with gelatin on preventing tendon adhesions following flexor tendon repair using a novel turkey animal model both in vitro and in vivo. We hypothesized that pentamidine could effectively reduce adhesions and improve limb function. We further hypothesized that the optimized dose of pentamidine could eliminate an adverse effect of impairing tendon healing.

2. Materials and methods

2.1. Study design

To test our hypotheses, we used both in vitro and in vivo models to characterize pentamidine effectiveness. In the in vitro model, we used turkey tenocytes that were harvested from turkey flexor tendons for cellular and molecular assessments with various pentamidine doses that were based on the range of clinical use and our rabbit wound healing pilot study from 0 to 100 ug/ml. The optimal dose was considered to be the maximal does of pentamidine that did not significantly decrease cell proliferation, migration, adhesion, and collagen production. Then, pentamidine at the selected optimal dose was embedded with 10 % gelatin to fabricate a pentamidine-sheet, and the pentamidine-sheet was then validated in an in vivo turkey flexor tendon model. At six weeks follow up, turkeys were sacrificed for the evaluations described in detail below.

2.2. In vitro experiment

2.2.1. Isolation and culture of Turkey tenocytes

Two flexor digitorum profundus (FDP) tendons from one heritage-breed turkey (6 months, weighing 8–10 kg) were used for the isolation of tenocytes. The turkey tendon model is a well-established large animal model for flexor tendon injury [6,18]. The turkey for tenocyte isolation was killed for another IACUC-approved project that did not involve tendon related research. Briefly, following removal of the connective tissue, the tendon was cut into approximately 1 mm^3 and incubated for 40 min in 5 ml 0.05 % collagenase. After being washed 3 times in PBS, the turkey tenocytes were cultured in Dulbecco's Modified Eagle's Medium (DMEM; Corning, USA) supplemented with 10 % fetal bovine serum (FBS; Gibco®, USA) and 1 % antibiotic–antimycotic (AA; Gibco®, USA) in a humidified incubator containing 5 % CO2 at 37 °C. After a second passage, all the above cells were used for the following experiments.

2.2.2. Gelatin concentration test

Before the cell experiment, optimal dosages of gelatin (Sigma, USA) and pentamidine (HIPAASpace, USA) were validated according to previous studies [19–21]. In brief, turkey tenocytes were seeded 2×10^4 cells per well on a 12-well plate (Corning®, USA) and incubated at 37 °C for 24 h to permit complete adhesion. The groupings were as the following: 10 % gelatin with/without 50 μg/mL pentamidine, 20 % gelatin with/without 50 μg/mL pentamidine, respectively (Supplemental Fig. 1). Subsequently, the cells viability of each group was captured in real-time by using IncuCyte® S3 Live Cell Analysis System (Essen BioScience, USA).

2.2.3. Cell viability assay

To explore the dose effect of pentamidine, the tenocytes were divided into groups based on different concentrations of pentamidine (0, 5, 10, 15, 20, 25, 30, 35, 40, 45, and 50 μg/mL). Turkey tenocytes were prepared by seeding 1×10^3 cells per well on a 96-well plate (Corning®, USA) and incubated at 37 °C for 24 h to permit complete adhesion. Subsequently, cellular viability of each group was captured in real-time and analyzed by using IncuCyte® S3 Live Cell Analysis System (Essen BioScience, USA).

2.2.4. Cell migration assay

For the cell migration assay, turkey tenocytes were seeded with 1×10^4 cells per well on a 12-well plate (Corning®, USA) and incubated at 37 °C for 24 h to permit complete adhesion. A scratch was introduced to the confluent cells with a 200-μL sterile pipette tip (Molecular BioProducts, USA). Turkey tenocytes were allowed to continue growing for 48 h in different pentamidine dose groups (0, 10, 20, 30, 40, and 50 μg/mL). Similarly, the cell migration of each group was captured in real-time by using IncuCyte® S3 Live Cell Analysis System (Essen BioScience, USA) and the cells migrating rate was analyzed by Image J Software (v.1.8.0, NIH, USA).

2.2.5. Live and dead cell assay

The live and dead cell assay was performed using a LIVE/DEAD™ Viability/Cytotoxicity kit (ThermoFisher, USA) according to the manufacturer's instructions. In brief, Turkey tenocytes were seeded with 1×10^4 cells per well on a 12-well plate (Corning®, USA) and incubated at 37 °C for 24 h to permit complete adhesion. Turkey tenocytes were allowed to continue growing for 48 h in different concentrations of pentamidine (0, 5, 10, 15, 20, 25, 30, 35, 40, 45, 50, and 100 μg/mL). After 24 h, Calcein AM (1:2000) and Ethidium homodimer-1 (1:500) were added to each well and incubated for 10 min. Subsequently, the fluorescence images of each well were captured and assessed in real-time by using IncuCyte® S3 Live Cell Analysis System (Essen BioScience, USA).

2.2.6. Cell adhesion assay

The cell adhesion assay was performed using a Cell Adhesion kit (Cell Biolabs, USA) according to the manufacturer's instructions. Briefly, Turkey tenocytes were seeded with 2×10^3 cells per well on a 48-well plate and incubated at 37 °C for 1 h to permit complete adhesion. The media of each well was carefully aspirated and washed with phosphate buffered saline (PBS, ThermoFisher, USA) for 4–5 times. After incubated with Lysis Buffer/CyQuant® GR dye solution for 20 min at room temperature with shaking. The fluorescence of each well was read and assessed with a plate reader (BMGLABTECH, USA) at 480/520 nm.

2.2.7. Pentamidine-gelatin sheet preparation

In order to deliver pentamidine in our flexor tendon repair in vivo model, we used 10 % gelatin, which has been used for flexor tendon surface modification in many studies [22–24], to fabricate a

pentamidine-gelatin sheet. The optimal dose of pentamidine was 25 ug/mL based on the in vitro optimization experiments. The MES solution was prepared through mixing MES hydrate (Sigma, USA) and saline, using digital pH meter to adjust the pH to 6.0 with either NaOH or HCL (all from Sigma, USA). The pentamidine isethionate solution was prepared by mixing pentamidine powder into saline. The gelatin solution was prepared by adding gelatin powder to the MES solution and stirred at 80 °C until clear. The gelatin solution was cooled to 45 °C, and the pentamidine solution was added into the gelatin solution while stirring continuously for 5 min to achieve the desired concentration (25 ug/mL pentamidine and 10 % gelatin). The final pentamidine-infused gelatin was poured onto silver paper, cooling it to room temperature until it became a gel.

2.2.8. Scanning electron microscopy (SEM) of pentamidine-gelatin sheet

The gelatin patches with or without pentamidine were dehydrated in increasing concentrations of alcohol (70 %, 80 %, 90 %, and 100 %) and were critically dried with a CO2 critical-point dryer. They were mounted onto aluminum stubs and coated with gold, then viewed under a scanning electron microscope (SEM) at an accelerating voltage of 3.0 kV.

2.2.9. In vivo experiment

2.2.9.1. Ethics statement. Thirty female adult Red Bourbon turkeys (about 1 year old, weighing 8–10 kg) were randomly assigned into three groups: Control (surgery only), Gelatin (surgery with 10 % gelatin sheet alone), or Pentamidine (surgery with pentamidine gelatin sheet) with 10 turkeys per group. The experimental procedures and animal care were approved by our Institutional Animal Care and Use Committee (IACUC No. A00003525-18). Before surgery, all turkeys were kept under a humidity- and temperature-controlled environment with free access to food and water.

2.2.10. Animal model

The third (middle) digit on either the right or left foot of each turkey was randomly chosen to be surgically repaired. The other non-operated third digit served as the baseline. A Z-shaped incision was made at the level of the proximal interphalangeal (PIP) joint on the volar side of the third digit. The flexor digitorum profundus tendon was exposed and a laceration was made 1 cm distal to the proximal vinculum. Tendon was repaired with the modified Pennington technique (4-0 Fiberwire) and a circumferential running suture (6-0 Prolene). After tendon repair, the skin was closed with 3-0 Vicryl sutures. All operated feet were wrapped with gauze and cast with digits in flexion until sacrifice six weeks after surgery. Following animal sacrifice, the repaired digits, and tendons were tested for work of flexion (WOF), tendon gliding resistance, and repair strength, as well as assessed by real-time quantitative reverse transcription polymerase chain reaction (qRT-PCR), histology, and immunohistochemistry.

2.2.11. Adhesion score

All the repaired tendons were dissected and scored at based on a previously published scoring system of 0 (no adhesion) to 4 (severe adhesions) [18,25]. The scorers (SG and KN) were blinded to the treatments. Scoring occurred at two sites making the total score from 0 to 8.

2.2.12. Normalized work of flexion (nWOF)

Work of flexion at the PIP joint was assessed in eight turkeys in each group with a combined tensile transducer and a motion analysis system as previously described [26–28]. Briefly, a Kirschner wire was inserted longitudinally through the most proximal phalangeal bone. Reflective markers were attached to the distal phalanx in turkey to serve as markers for the phalanges. The prepared digit was mounted on the testing device by fixing the proximal Kirschner wire (K-wire) to a custom jig. The testing device consisted of a testing frame, actuator, linear potentiometer, and one load transducer. A 0.5-N weight was attached to the extensor tendon to ensure full extension of the digit as a starting position and to apply an initial tension to the flexor tendons. The actuator pulled the tendon proximally at a rate of 2 mm/s, causing digital flexion, until the digit was fully flexed. Data from the linear potentiometer and proximal load transducer were recorded at 50 Hz. During testing, digit marker motion (from extension to flexion) was recorded simultaneously by motion capture cameras (Motion Analysis Corp., Santa Rosa, CA) to obtain PIP and DIP joint motion. The total work of flexion was calculated based on the area of force–displacement curve, and nWOF was calculated by total WOF divided by total PIP and distal interphalangeal (DIP) joint motion angles, which indicated the work to move joint per degree.

2.2.13. Measurement of tendon gliding resistance

Following the WOF measurement, the tendon graft was further dissected, with the proximal pulley kept intact. The gap size of repaired tendons was also evaluated with calipers. The proximal pulley and tendon repair site were then measured with use of a custom tendon-pulley frictional testing device according to previous studies [27,29]. In brief, the FDP tendon and proximal pulley were preserved after dissection. The proximal phalanx was mounted on the device with the K-wire that had been used to fix the metacarpophalangeal joint. One mechanical actuator with a linear potentiometer was connected to the proximal end of the FDP tendon. The custom-made ring load transducer and a 500 g weight were connected to the distal end of the FDP tendon. The tendon was pulled proximally by the actuator against the weight at a rate of 2 mm/s. The force differential between the proximal and distal tendon ends represents the gliding resistance.

2.2.14. Measurement of repair strength

After tendon gliding test, eight repaired tendons in each group had mechanical strength testing according to previously published protocols [26,27]. Briefly, the FDP tendons were secured to a servo hydraulic testing machine (MTS Systems, Eden Prairie, Minnesota) and distracted to failure at a rate of 20 mm/min. A differential variable reluctance transducer (MicroStrain, Williston, Vermont) was attached to the repair site of the FDP tendon through two barbed pins inserted perpendicularly into the tendon to measure gap formation during testing. The repair strength and stiffness (the slope of force versus displacement) at the repair site were measured to assess the mechanical quality of healing of the repaired tendon.

2.2.15. Bioinformatic analysis

In order to further explore the molecular changes in the WNT signaling pathway after tendon injury and the effect of pentamidine on them, based on the similarity of tendon peritendinous adhesion in both turkey and human tendon injury, we used the National Centre of Biotechnology Information (NCBI) Gene Expression Omnibus database. In this database, human tendon samples were collected, and total RNA was isolated at 2–3 weeks after injury. The transcriptome profiles of GSE108933 were obtained from the NCBI, which comprises a total of 6 samples, including 3 injury tendon tissues (peritendinous fibrosis) and 3 normal tendon tissues [30]. All differentially expressed genes (DEGs) were imported into GraphPad Prism Software (GraphPad v8.2, CA) and Cytoscape Software (v3.8.2) for data analysis and statistical analysis. Then all DEGs were used for subsequent functional enrichment analysis of Gene Ontology (GO) analysis using DAVID (the Database for Annotation, Visualization, and Integrated Discovery, https://david.ncifcrf.gov/2021.02.15).

According to the GSE108933 database, a total of 20325 DEGs were detected with significant differences between injured tendons and normal tendons. Of these 20325, 131 DEGs were identified as Wnt related genes. The chromosomal distribution of these 131 DEGs is shown in Fig. 5A. The results of GO enrichment analysis are presented in

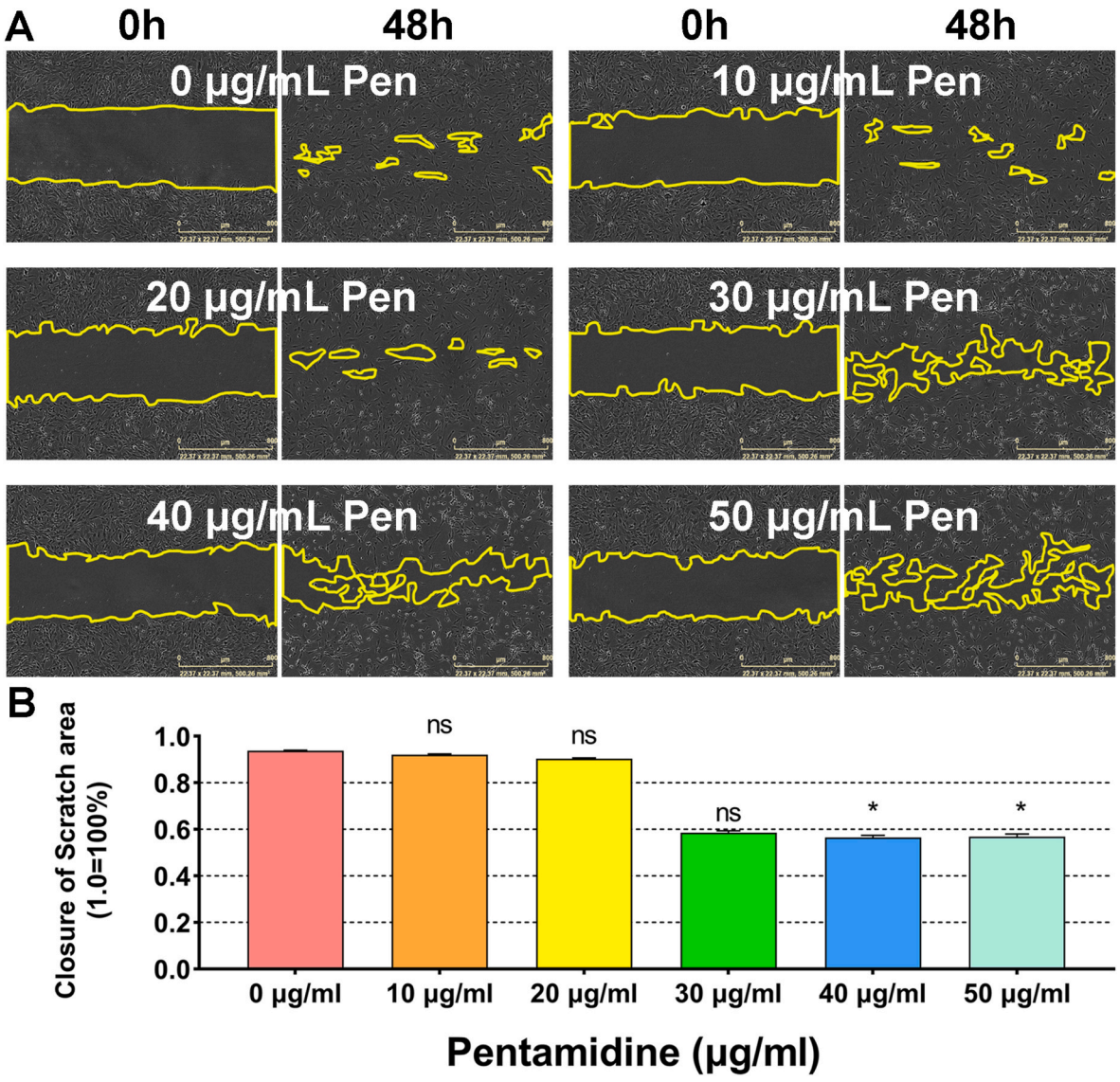

Fig. 1. The cell migration test of pentamidine in turkey tenocytes. (**A**) The overview of turkey tenocytes treated with different doses of pentamidine (0–50 μg/mL) at 0 h to 48 h in IncuCyte® S3 Live Cell Analysis System. Scale bar: 800 μm. (**B**) The cell migration test showed the 40 and 50 μg/mL pentamidine groups could significantly reduce the cell migration compare with 0 μg/mL pentamidine groups at 48 h post-seeded.*p < 0.05, **p < 0.01, ***p < 0.001, ****p < 0.0001.

Fig. 5B. We found that these DEGs were mainly associated with terms related to the WNT signaling pathway, protein binding, and nucleoplasm. The PPI network of 131 Wnt related DEGs for tendon injury are shown in Fig. 5C. All of the 131 Wnt related DEGs are shown in a heat map (Fig. 5D).

2.2.16. RNA isolation and qRT-PCR

Total RNA was extracted from turkey tendons with TRIzol (Invitrogen, USA). Following RNA extraction, 1 μg of total RNA per sample was reverse transcribed using the iScript™ cDNA Synthesis Kit (Bio-Rad, USA). In addition, the thermal program consisted of 2 min at 95 °C, then 40 cycles of amplifications, 5 s at 95 °C for denaturation, 5 s at 65 °C for annealing, and 5 s at 95 °C for extension. All samples were performed on C1000 Touch™ Thermal Cycler (Bio-Rad, USA) using SYBR Green PCR Master Mix (Quantabio, USA) to measure the gene expressions of collagen type I alpha 2 chain (COL1A2), collagen type II alpha 1 chain (COL2A1), SRY-box transcription factor 9 (SCX9), decorin (DCN), tenomodulin (TNMD), Wnt family member 3A (WNT3A), Wnt family member 5A (WNT5A), Wnt family member 7A (WNT7A), Wnt family member 9A (WNT9A), Wnt family member 11 (WNT11), Wnt family member 16 (WNT16), and teneurin-3-like (Teneurin3). GAPDH and RPL19 were used as the internal control and all the primers are shown in Supplemental Table 1. Each sample was analyzed in triplicate. The relative quantification of the genes of interest was calculated using the $2^{-\Delta\Delta Ct}$ method.

2.2.17. Histological evaluation

For histology, two turkeys in each group were used for histological evaluation and immunohistochemistry. Briefly, tendon tissues in each group were prepared as paraffin sagittal sections at 5 μm thickness. Sections were stained with Hematoxylin and Eosin (Thermo Fisher Scientific, USA), Sirius Red (Polysciences, USA), and Masson staining (American Mastertech Scientific, USA) to evaluate the morphology and cellularity with light microscopy (Zeiss, Germany).

2.2.18. Immunohistochemistry

For immunohistochemistry, sections were stained with Collagen Type I (COL1) antibody (Catalog No. ABIN5680216, Antibodies, USA), Collagen Type III (COL3) antibody (Catalog No. ABIN237035, Antibodies, USA), WNT7A (Catalog No. ABIN1049483, Antibodies, USA)

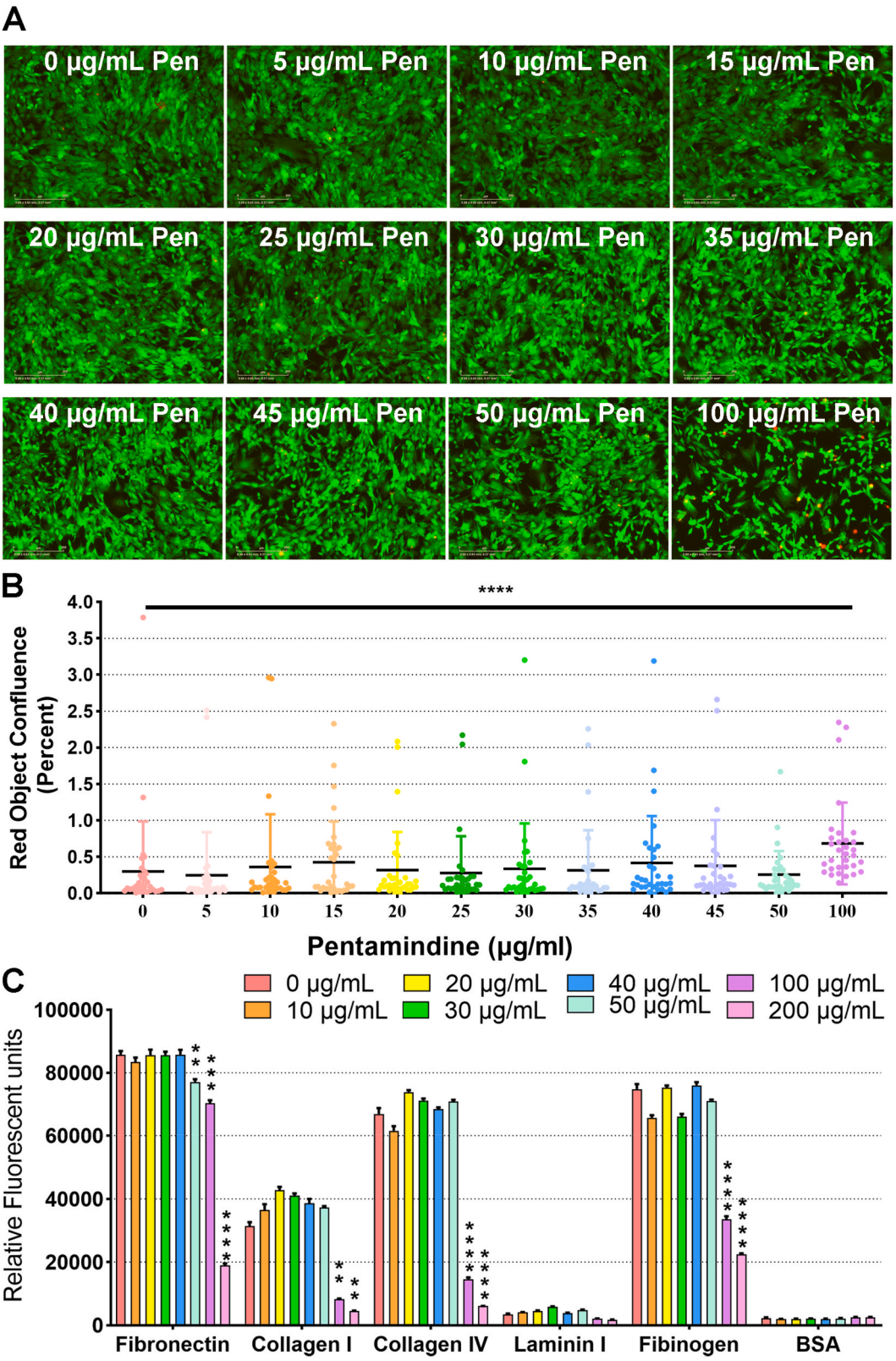

Fig. 2. The live/dead and adhesion assay of pentamidine in turkey tenocytes. (**A**) Tenocytes viability was assessed and visualized by live/dead assay with fluorescent dyes to distinguish live (green) and dead cells (red) at 24 h post-seeded in IncuCyte® S3 Live Cell Analysis System. Scale bar: 200 μm. (**B**) The quantitative analysis showed high dose of pentamidine (>45 μg/mL) could significantly reduce the cell viability compare with 0 μg/mL pentamidine group. (**C**) The cell adhesion assay showed 100–200 μg/mL pentamidine could significantly reduce the cell adhesion compare with 0 μg/mL pentamidine at Fibronectin, Collagen I, Collagen IV, and Fibrinogen groups. BSA group was as a negative control. *$p < 0.05$, **$p < 0.01$, ***$p < 0.001$, ****$p < 0.0001$. (For interpretation of the references to color in this figure legend, the reader is referred to the Web version of this article.)

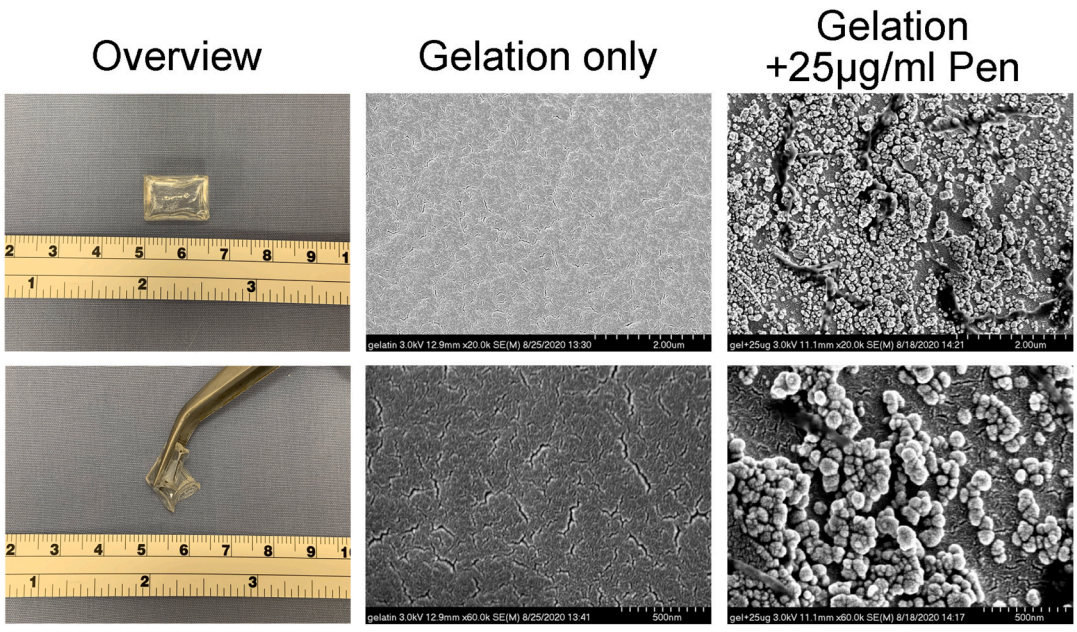

Fig. 3. The overview and SEM of pentamidine-gelatin patch. The scan electron microscopy showed the patch of gelatin only group had a smooth surface without particles. While the gelatin patch with 25 μg/mL pentamidine group had a rough surface with many pentamidine particles clustered together.

and WNT11 antibody (Catalog No. ABIN1049471, Antibodies, USA). Then, the sections were stained with Alexa Fluor 488-conjugated AffiniPure Goat Anti-Rabbit IgG (H + L) (1:200, Jackson ImmunoResearch, USA), AffiniPure Donkey Anti-Rabbit IgG (H + L) (1:200, Jackson ImmunoResearch, USA), and DAPI (1:100, Thermo, USA), respectively. The quantification of COL1, COL3, WNT7A, and WNT11 positive areas was evaluated with 6 non-overlapping randomly areas per specimen under the confocal (Zeiss, Germany). The positive rate was analyzed by Image J Software (v.1.8.0, NIH, USA).

2.2.19. Statistical analysis

All data are presented as the mean ± SEM. Statistical analysis was performed with GraphPad Prism statistical software (version 8.0.2; GraphPad Software, Inc., San Diego, CA); the For multiple comparisons, one-way analysis of variance (ANOVA) was used to detected significant differences followed by Tukey's multiple comparisons test to compare differences between two groups. The Kruskal–Wallis test was performed when the data is not a normal distribution. p values less than 0.05 were considered statistically significant.

3. Results

3.1. In vitro experiment

An in vitro dose test was performed with turkey tenocytes to evaluate the dose of pentamidine and gelatin use. In this study, turkey tenocytes were treated with different doses of gelatin (10 % or 20 %) with or without pentamidine (50 μg/mL) and captured in real-time by using IncuCyte® S3 Live Cell Analysis System. Supplemental Fig. 1 shows that 50 μg/mL pentamidine significantly reduced the cell viability ($p < 0.05$) compared with no pentamidine groups at days 5, 6, 7, 8, and 9 post-seeding. There was no significant difference between the 10 % 20 % gelatin groups ($p > 0.05$).

3.1.1. Effect of pentamidine on tenocyte proliferation and migration

The cell viability test showed there was no significant difference between the 0–25 μg/mL pentamidine groups ($p > 0.05$). However, 30–50 μg/mL pentamidine resulted in significantly reduced cell viability ($p < 0.05$) compared with 0 μg/mL pentamidine at days 5 and 6 following cell seeding (Supplemental Fig. 2). Cell migration assay showed no significant difference between the 0–30 μg/mL pentamidine groups ($p > 0.05$), but 40 and 50 μg/mL pentamidine doses significantly reduced cell migration ($p < 0.05$) at 48 h post-seeding (Fig. 1A and B). In addition, the live and dead test showed that 45 μg/mL pentamidine ($p < 0.05$) and 100 μg/mL pentamidine ($p < 0.0001$) significantly reduced cell viability compare with 0 μg/mL pentamidine group (Fig. 2A and B).

3.1.2. Pentamidine reduced Turkey tenocyte adhesion

The cells treated with different doses of pentamidine were mixed with Fibronectin, Collagen I, Collagen IV, Laminin I, Fibrinogen, or Bovine Serum Albumin (BSA). BSA was a negative control. As shown in Fig. 2C, the cell adhesion test showed there was no significant difference among different doses of pentamidine in Laminin I and BSA groups. However, 100–200 μg/mL pentamidine significantly reduced the cell adhesion ($p < 0.01$) compare with 0 μg/mL pentamidine in the Fibronectin, Collagen I, Collagen IV, and Fibrinogen groups. In the Fibronectin group, 50 μg/mL pentamidine also significantly reduced the cell adhesion ($p < 0.01$) compared with 0 μg/mL pentamidine.

3.1.3. Characterization of pentamidine-gelatin patch

As shown in Fig. 3, the pentamidine-gelatin patch is translucent, and the texture is soft and jelly-like. The size of the pentamidine-gelatin patch is about 1.5 cm (Long) × 1.0 cm (Short) × 0.5 cm (Thickness). The total volume of the pentamidine-gelatin patch is 1 mL. The SEM showed that the gelatin sheet alone had a smooth surface. However, the gelatin patch with 25 μg/mL pentamidine had a rough surface with many pentamidine particles clustered together.

3.2. In vivo experiment

3.2.1. Adhesion formation and WOF

As shown in Fig. 4A, the suture method of tendon repair was a modified Pennington technique (Red line) with a circumferential running suture (Green line). The surgical procedure and casting process were performed according to the above descriptions (Fig. 4B and C). The circle in Fig. 4B showed the area of the material placement. Six weeks later, after dissection of all FDP tendons, all tendons in each group were intact and the overview of the surface is shown in Fig. 4D. For the

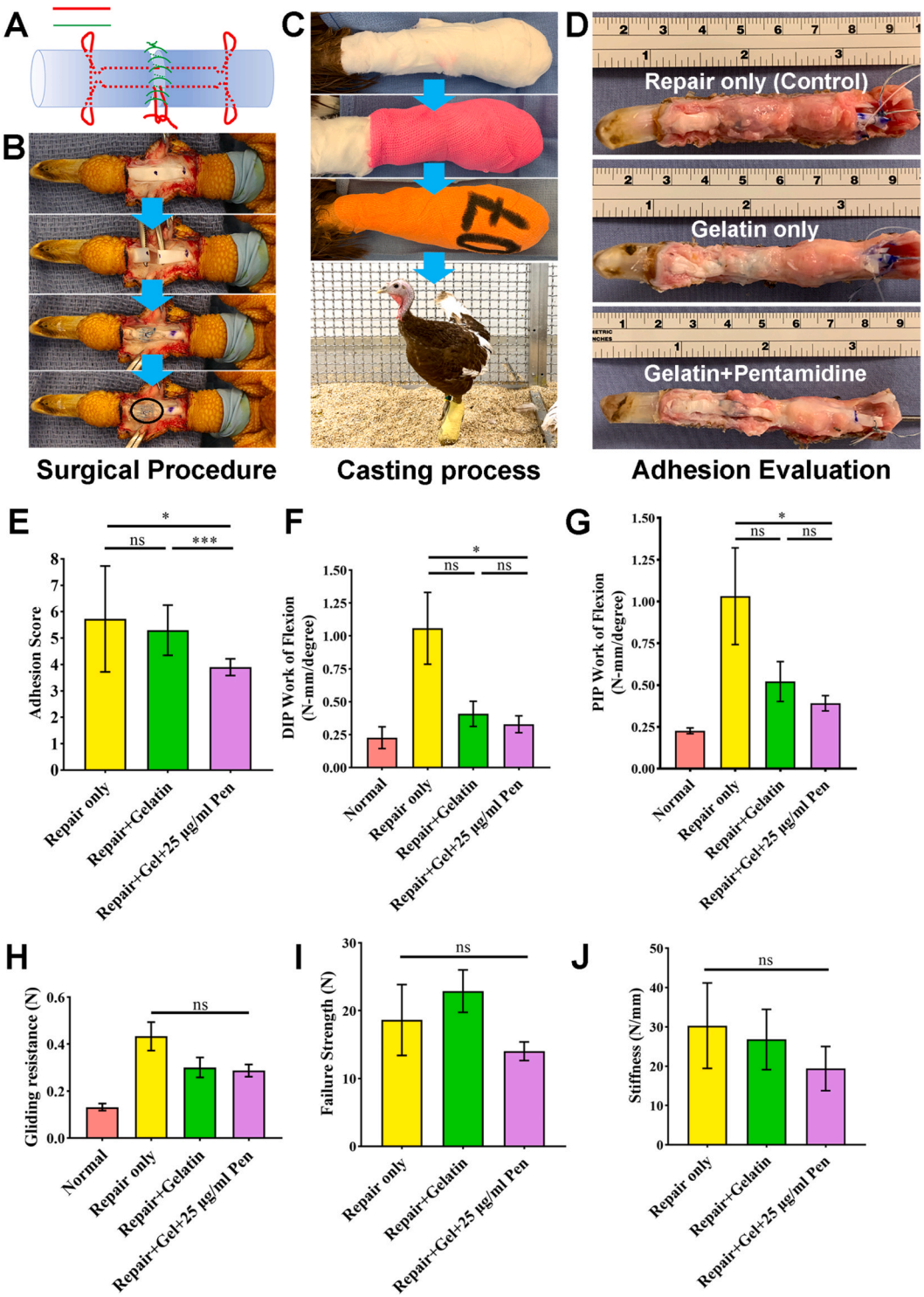

Fig. 4. Pentamidine-gelatin patch decreases adhesion formation and WOF after flexor tendon repair. (**A**) The suture method of tendon repair was modified Pennington technique (Red line) with circumferential running suture (Green line). (**B, C**) The surgical procedure and casting process of *in vivo* study. (**D**) The overview of the surface of FDP tendon. (**E**) The adhesion score in Pentamidine group was significantly lower than that in Control group and Gelatin group. (**F, G**) WOF in the Pentamidine group was significantly lower than that in the Control group. (**H**) No difference was found in frictional force among each group. (**I, J**) No difference was found in frictional force among each group. *p < 0.05, **p < 0.01, ***p < 0.001, ****p < 0.0001. (For interpretation of the references to color in this figure legend, the reader is referred to the Web version of this article.)

adhesion score, no difference was found between the Control and Gelatin groups ($p > 0.05$), while the adhesion score in the Pentamidine group was significantly lower than that in the Control group ($p < 0.05$) and Gelatin group ($p < 0.001$) (Fig. 4E).

For the work of flexion, both the distal interphalangeal and the proximal interphalangeal of WOF in the Pentamidine group were significantly lower than that in the Control group ($p < 0.05$), while there was no difference between the Control and Gelatin groups ($p > 0.05$) or Gelatin and Pentamidine groups ($p > 0.05$) (Fig. 4F and G). For the gliding resistance, no difference was found in frictional force between

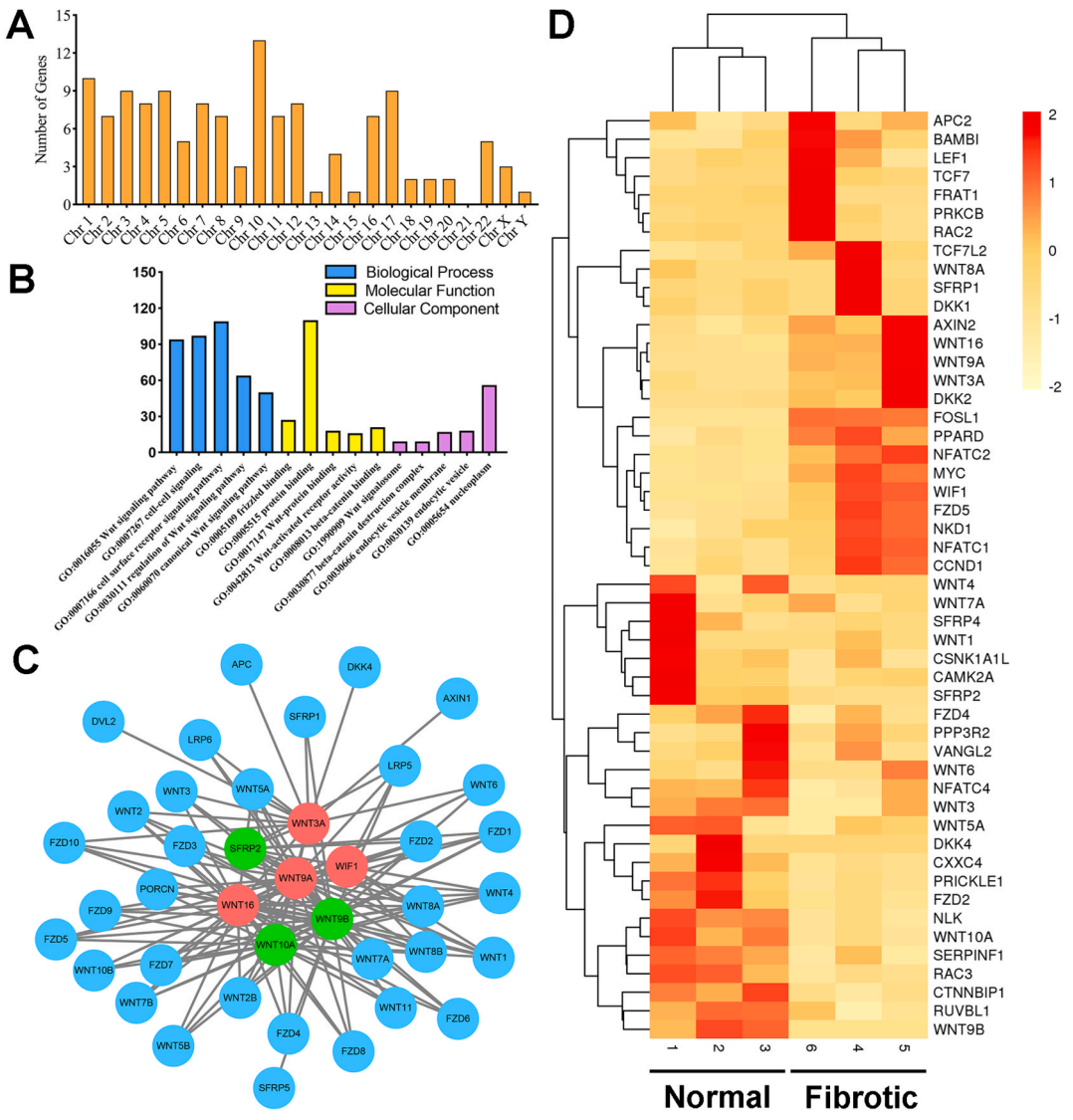

Fig. 5. Expression signatures of differential expression genes in injury tendons and normal tendons. (**A**) Chromosome distribution showed the numbers of differential expression genes located at different chromosomes. (**B**) GO analysis of differential expression genes. BP, biological processes; CC, cellular component; GO, gene ontology; (**C**) PPI network and the core genes of the differential methylation genes. (**D**) Representative heat map of the 131 Wnt-related differential expression genes.

the 3 groups ($p > 0.05$) (Fig. 4H). For the maximum strength to failure (Fig. 4I) and stiffness to failure, no difference was found in frictional force among the 3 groups ($p > 0.05$) (Fig. 4J).

3.2.2. Gene analysis by qPCR

To further verify the expression of these DEGs, gene expression was assessed by qPCR in vivo and in vitro. *In vitro* experiments (turkey tenocytes) showed the expression of WNT3A, WNT5A, WNT9A, WNT11, and Teneurins-3 to be significantly decreased in the Gelatin plus 100 μg/mL Pentamidine group compared to the Control group ($p < 0.05$) (Fig. 6A). For the expression of WNT7A and WNT16, there were no significant changes between the Gelatin plus Pentamidine group and Control group ($p > 0.05$). In tendon tissues, the expression of WNT3A, WNT5A, WNT7A, WNT9A, WNT11, WNT16, and Teneurins-3 was significantly decreased in the Gelatin plus 25 μg/mL Pentamidine group compared to the Control group ($p < 0.01$) (Fig. 6B). There were no significant changes in COL1A2, COL2A1, DCN, SCX, and TNMD expression among each group ($p > 0.05$) (Fig. 6C).

3.2.3. Histology and immunohistochemistry

Histologically, all tendons displayed complete healing with no visible gaps between the repaired tendon ends at day 42. Cellularity at the repair site seems not obviously different among different groups in H&E staining. Masson trichrome staining showed repaired tendon structure with randomly aligned collagen fibers. The Sirius red staining showed most of the collagen fibers belonged to type I collagen and difference in collagen alignment was observed (Fig. 7). Immunohistochemical staining found no differences in COL1A1 and COL2A1 among each group ($p > 0.05$). However, the expression of WNT7A and WNT11 was significantly decreased in the Pentamidine group when compared to Control ($p < 0.05$) and Gelatin groups ($p < 0.01$) (Fig. 8).

4. Discussion

The hypothesis of this study was supported that pentamidine-gelatin sheet significantly decreased adhesion formation after flexor digitorum profundus tendon repairs up to six weeks postoperatively, leading to improved digital function compared with that of the repaired tendon without pentamidine treatment. Pentamidine is an FDA-approved drug used to treat parasitic infections [31]. Early studies have shown that despite potentially serious side effects (nephrotoxicity, hypoglycemia, etc.), pentamidine can resolve pneumonia episodes in approximately

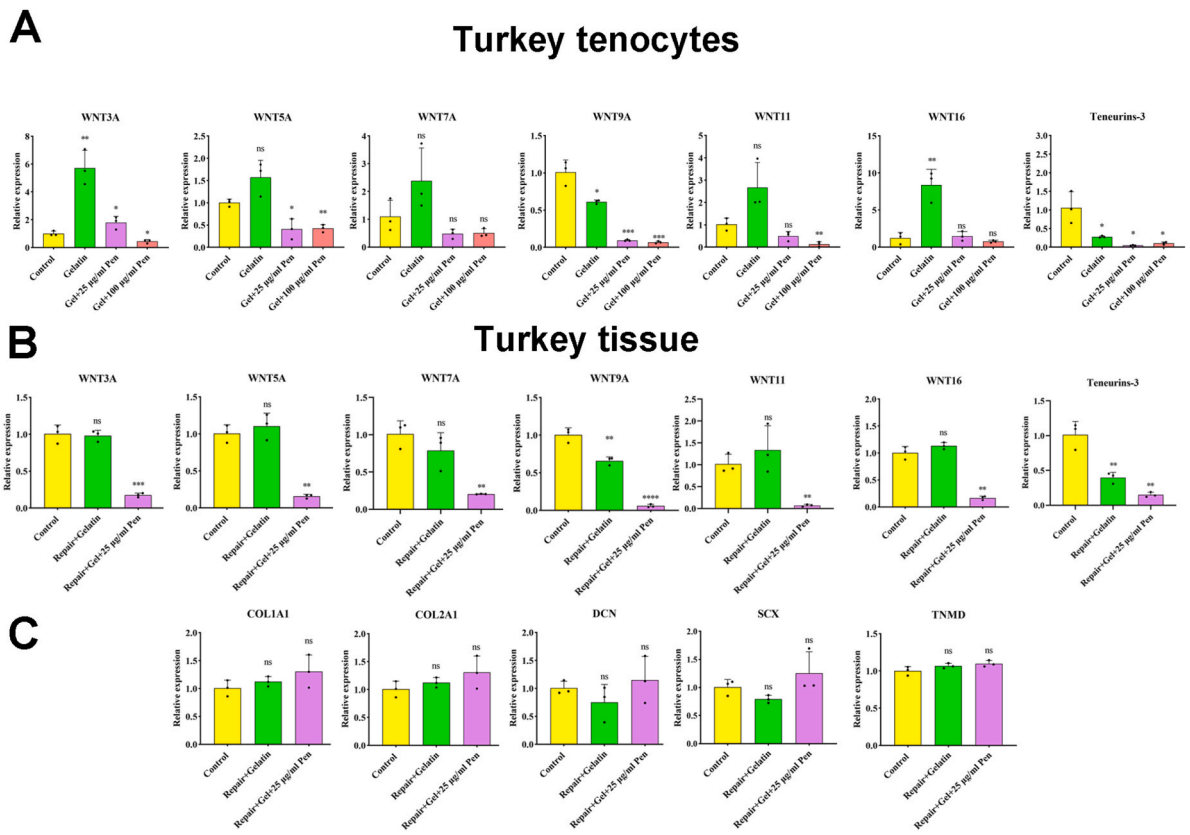

Fig. 6. Validation of the differential expression genes identified in bioinformation analysis by qRT-PCR. (**A**) The expression of Wnt-related differential expression genes in turkey tenocytes. (**B**) The expression of Wnt-related differential expression genes in turkey tissue with different treatments. (**C**) The expression of collagen-related genes in turkey tissue with different treatments. *$p < 0.05$, **$p < 0.01$, ***$p < 0.001$, ****$p < 0.0001$.

41–87 % of patients. It is a rigorously validated antibacterial agent, especially in the treatment of PCP in AIDS patients [32]. In our study, we have shown for the first time that a pentamidine-loaded gelatin scaffold can significantly reduce adhesions during tendon healing in an animal model.

As pentamidine is often systematically used in clinics with intravenous and intramuscular injection, the effective dose for localized application in tendon repair needed to be defined. During our pilot experiment, we used 300 mg pentamidine powder, which is the typical clinical dose, directly applied to the repaired tendon that resulted in all repaired tendons being ruptured at six weeks. This failed experiment indicates the strong anti-proliferative effects of pentamidine, through interference of critical functions in DNA, RNA, phospholipid, and protein synthesis. Therefore, various concentrations of pentamidine were studied using an in vitro model, to identify an appropriate level for use to block tendon adhesions. We selected a range to screen for the optimal dose, one that would not negatively affect tenocyte viability, proliferation, or migration. The dose of 25 ug/mL, though far lower than the clinical dosed used as an antibiotic, demonstrated effectiveness in reducing adhesions and improving digit function after tendon repair in our vivo experiment. Further bioinformatics analysis, qPCR, and IHC verified that the possible mechanism of pentamidine reducing tendon adhesion may be due to the significant reduction of Wnt7A and Wnt11 in the WNT signaling pathway.

Many different materials have been tried to prevent or reduce adhesions during tendon healing, including ubricants, growth factors, and physical barriers. The effective components of them include carbodiimide-derivatized hyaluronic acid [33], gelatin [34], lubricin [35], silver nanoparticles [36], and polylactic-co-glycolic acid (PLGA) [37]. All these require some sort of carrier, often a gelatin. Gelatin is an FDA-approved hydrogel in which has been used in tissue engineering [38], drug delivery [39], and regenerative medicine [40] due to its weak antigenicity [41], good biodegradability [42], and excellent biocompatibility [43]. Recently, Zhang et al. investigated platelet-rich plasma (PRP) combined with a gelatin sponge (GS) to improve tendon–bone interface healing and structure formation [44]. Bhavsar et al. evaluated the use of collagen-glycosaminoglycan (GAG) material as an adjunct to surgical for flexor tendon repair [45]. The study showed that collagen-GAG scaffold can effectively reduce formation of early postoperative tendon adhesions in chicken flexor tendon repair model without affecting the quality or strength of the tendon, mainly through the mechanism of physical barriers that protect tendon intrinsic healing and obstruct extrinsic healing. Previous studies showed that the degradation of collagen-GAG scaffold in vivo was usually 2–3 weeks [45]. In this study, after 6 weeks, the gelatin was completely degraded. However, the smaller number of experimental animals and shorter observation period are the limitations of this study. In this study, when we dissolved up to 100ug/L of pentamidine into the collagen-GAG scaffold, we did not find any precipitation or crystallization, and the encapsulation has good repeatability and easy operability. To our knowledge, this current study is the first to combine two FDA-approved drugs to create a bioactive scaffold with high histocompatibility and easily degradable in vivo, which can successfully reduce adhesions during tendon healing. All the above results were in good agreement, indicating the results are valid and repeatable.

The outcomes of previous studies regarding postoperative adhesion and functional recovery are similar to this study but ultimately failed to explain the mechanism why various composite scaffolds can reduce postoperative tendon adhesion [46–48]. After discovering that the pentamidine-gelatin scaffold can reduce the adhesion after tendon repair, we investigated the GEO database (GSE108933) of NCBI, and revealed 20325 DEGs between normal tendon and injury tendon, and

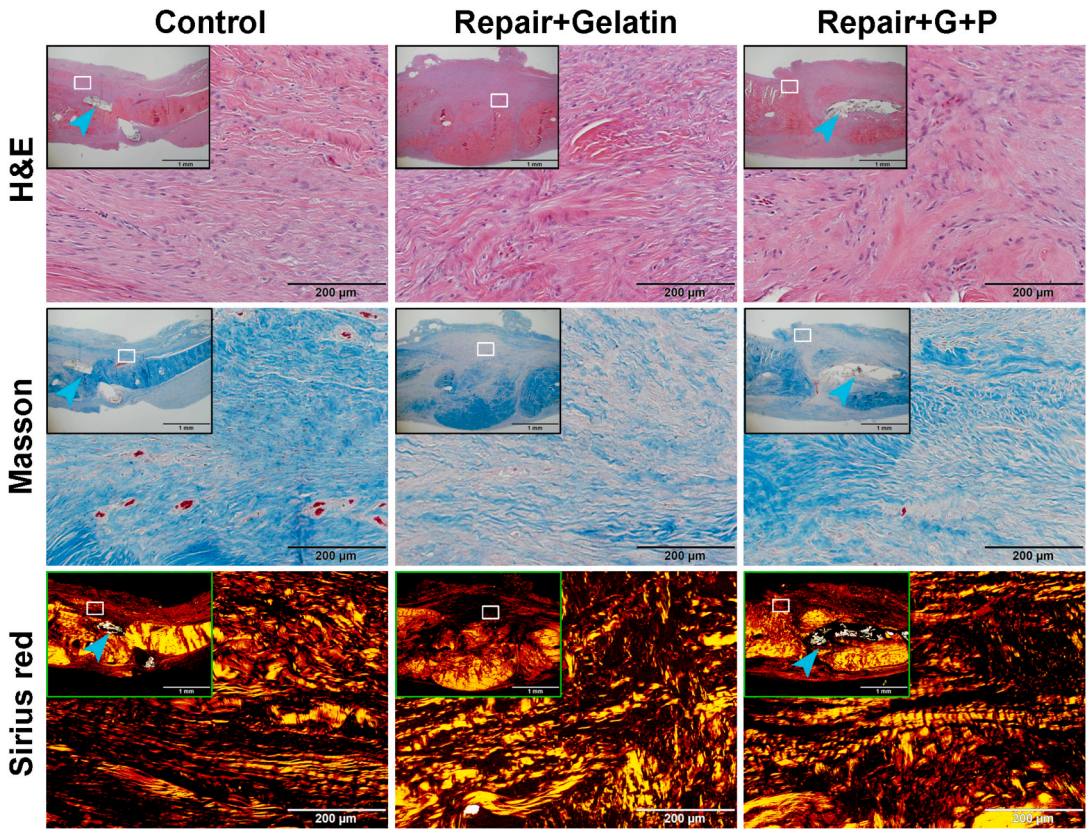

Fig. 7. Histology results of healing tendons in different groups at 6 weeks. (**A**) Representative H&E staining images at 6 weeks after surgery. (**B**) Representative Masson staining images at 6 weeks after surgery. (**C**) Representative Sirius red staining images at 6 weeks after surgery. Scale bar: 200 μm. Narrow showed running suture. (For interpretation of the references to color in this figure legend, the reader is referred to the Web version of this article.)

further identified important adhesion markers related to the Wnt signal pathway. A previous study demonstrated that the formation of flexor and extensor tendons of digits occurs between the surface of the ectoderm and differentiated phalanges, and the formation of the tendons of the ectoderm is related to the expression of Wnt family members, including Wnt6, Wnt7a, and Wnt3 [49,50]. In addition, multiple previous studies have shown that there is a close relationship between several Wnt members and adhesion, including Wnt3a, Wnt5a, Wnt7a, and Wnt11 [51,52]. Yoshioka et al. found that Wnt7a expression could affect cell proliferation, adhesion, and invasion in vitro analysis of cell function [53]. They demonstrated that the high expression of Wnt7a can increase cell–cell adhesion and promote tumor cell proliferation, which is consentient with our findings that pentamidine reduced Wnt7a expression leading to decreased adhesion after tendon repair. In addition, Wnt11 also plays an important role in cell–cell adhesion [54–56]. Besides cell adhesion, the Wnt pathway was reported to suppress tenogenic genes of Scx, Mkx, and Tnmd [57,58]. Supressing the Wnt pathway was shown to reduce peritenous scars and improve tendon biomechanical functions [59–61].

This study had several limitations. First, tendon gap size was not measured in this study, all the in vivo experimental data were obtained at one time point, six weeks after repair. Second, the animals we used were only female turkeys, due to limited accessibility of male turkeys. However, since the tendon structure, cellular and molecular composition are similar between female and male, the comparison between different treatment groups should be reliable. We only discussed the role of tendon cells in the process of tendon regeneration. Third, the microenvironment of tendon regeneration in vivo is complex, and a variety of inflammatory cells, fibroblasts and tendon cells participate in and coordinate the repair of tendons. Fourth, we did not perform a drug release test for Pentamidine from the gelatin gel, a crucial aspect in pharmaceutical treatment development. A sustained and controlled release of pentamidine from the delivery system is a critical feature that impact its efficacy. Establishing and optimizing a new method to address this limitation will require a few months. While the primary focus of this paper centers on therapeutic outcomes and performance tests, investigating the release of Pentamidine from the gelatin will be our pivotal next step. Finally, although we did not detect significant failure strength differences among our three groups, a lack of difference might be related to the small sample size. The strength of pentamidine group showed a trend of decreased healing, which indicated tendon healing might be compromised by pentamidine treatment. Therefore, further investigation with a larger sample size and varied doses in a vivo model is needed before considering clinical translation.

In summary, this study for the first time discovered and tested a pharmaceutical antibiotic drug, pentaamine, for adhesion prevention after flexor tendon repair. Our results demonstrated that a pentamidine gelatin sheet effectively reduced adhesions and improve digit function after flexor tendon repair using a novel turkey model. The qPCR, histology, and immunohistochemistry further delineated the possible mechanism that decreased adhesion formation of pentamidine might have gone through regulating a Wnt signaling pathway. However, the trend of decreased healing by pentamidine raises a caution for clinical application, which needs further investigation.

Author contribution statement

G.S., designed the study, performed the experiments, acquired, analyzed and interpreted the data, and drafted the manuscript. N.K., T. H, P.A., A.M., C.Z. and S.M. contributed to study design, data interpretation, manuscript editing and finalizing the manuscript. Y.W., R.R., and A.W. also helped perform the experiments and analyzed the data. All

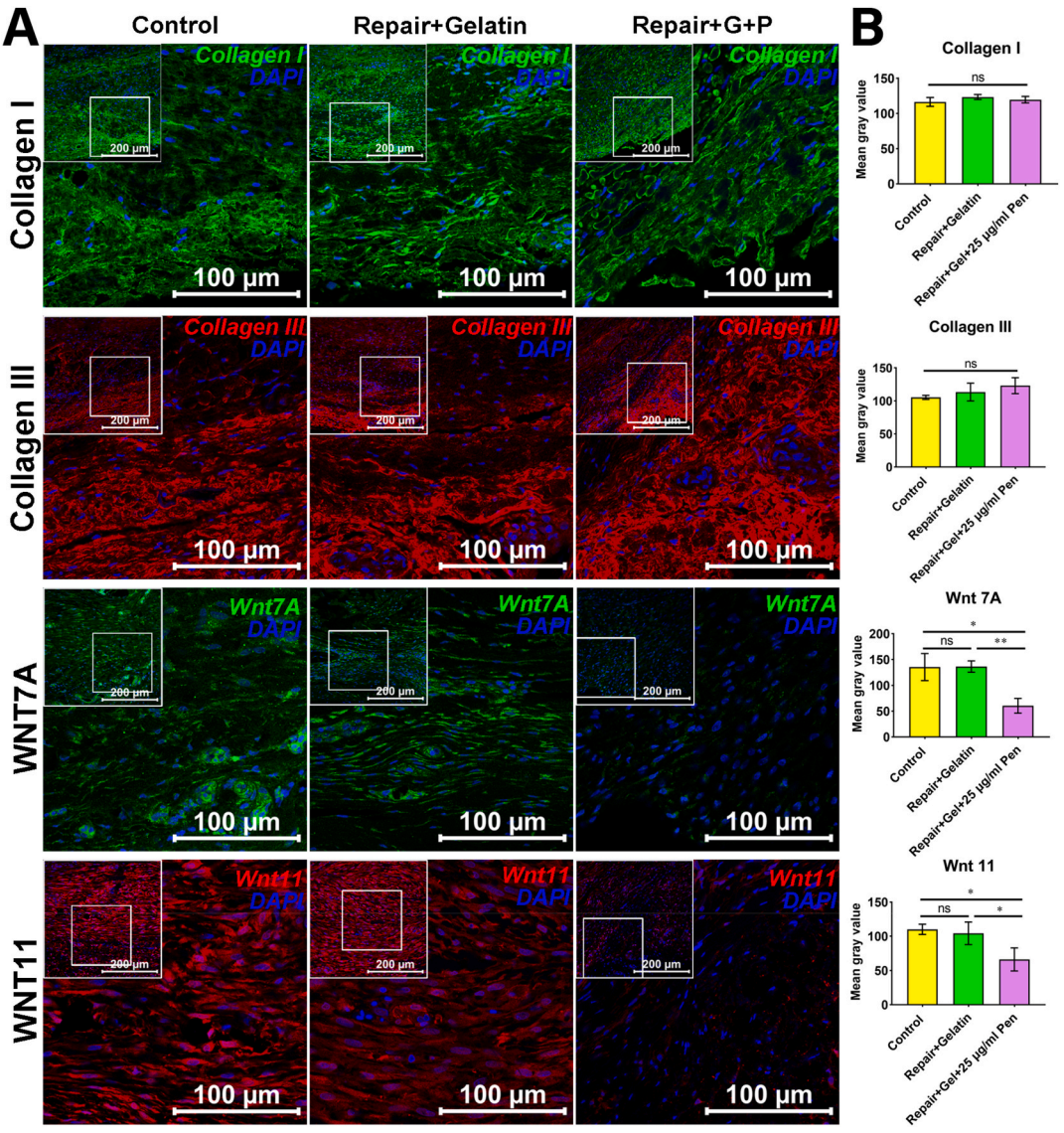

Fig. 8. Immunohistochemistry results of healing tendons in different groups at 6 weeks. (**A**) Immunofluorescence staining of COL1A2, COL3A1, Wnt7a, and Wnt11 at 6 weeks after surgery. (**B**) The quantitative analysis showed there were no significant changes in COL1A2 and COL3A1 among each group. However, the expression of Wnt7A and Wnt11 was significantly decreased in the Gelatin plus 25 μg/mL Pentamidine group compared to Control or Repair with Gelatin group. Scale bar: 100 μm *p < 0.05, **p < 0.01, ***p < 0.001, ****p < 0.0001.

authors have read and approved the final submitted manuscript.

Funding

This study was supported by grants from the Orthopedic Research Review Committee of Mayo Clinic [94064024], NIH NIAMS [AR57745], and the Mayo Clinic Kelly Fellow Award. The authors Guidong Shi and Zeling Long are funded by the China Scholarship Council. The author Guidong Shi is also funded by the postgraduate Innovation Fund of '13th Five-Year comprehensive investment' of Tianjin Medical University [YJSCX201903] and Tianjin Research Innovation Project for Postgraduate Students [2019YJSB109].

Declaration of AI and AI-assisted technologies

The authors declare that they didn't use any AI and AI-assisted technologies in the writing process.

Declaration of competing interest

The authors declare that they have no known competing financial interests or personal relationships that could have appeared to influence the work reported in this paper.

Acknowledgements

This study thanks the technical support from Ramona Reisdorf.

Appendix A. Supplementary data

Supplementary data to this article can be found online at https://doi.org/10.1016/j.jot.2023.10.007.

References

[1] Chesney A, Chauhan A, Kattan A, Farrokhyar F, Thoma A. Systematic review of flexor tendon rehabilitation protocols in zone II of the hand. Plast Reconstr Surg 2011;127(4):1583–92.

[2] Freeberg MAT, Farhat YM, Easa A, Kallenbach JG, Malcolm DW, Buckley MR, et al. Serpine1 knockdown enhances MMP activity after flexor tendon injury in mice: implications for adhesions therapy. Sci Rep 2018;8(1):5810.

[3] Zhao C, Zobitz ME, Sun YL, Predmore KS, Amadio PC, An KN, et al. Surface treatment with 5-fluorouracil after flexor tendon repair in a canine in vivo model. The Journal of bone and joint surgery American 2009;91(11):2673–82 [eng].

[4] Shi G, Wang Y, Wang Z, Thoreson AR, Jacobson DS, Amadio PC. A novel engineered purified exosome product patch for tendon healing: An explant in an ex vivo model. 2020. J Orthop Res 2021;39:1825–37. https://doi.org/10.1002/jor.24859.

[5] Zhao C, Hashimoto T, Kirk RL, Thoreson AR, Jay GD, Moran SL, et al. Resurfacing with chemically modified hyaluronic acid and lubricin for flexor tendon reconstruction. J Orthop Res : official publication of the Orthopaedic Research Society 2013;31(6):969–75 [eng].

[6] Kadar A, Thoreson AR, Reisdorf RL, Amadio PC, Moran SL, Zhao C. Turkey model for flexor tendon research: in vitro comparison of human, canine, Turkey, and chicken tendons. J Surg Res 2017;216:46–55 [eng].

[7] Yao Z, Wang W, Ning J, Zhang X, Zheng W, Qian Y, et al. Hydroxycamptothecin inhibits peritendinous adhesion via the endoplasmic Reticulum stress-dependent apoptosis. Front Pharmacol 2019;10:967 [eng].

[8] Dorlo TP, Kager PA. Pentamidine dosage: a base/salt confusion. PLoS Negl Trop Dis 2008;2(5):e225.

[9] Lin J, Yang QY, Yan Z, Markowitz J, Wilder PT, Carrier F, et al. Inhibiting S100B restores p53 levels in primary malignant melanoma cancer cells. J Biol Chem 2004;279(32):34071–7 [English].

[10] Markowitz J, Chen J, Gitti R, Baldisseri DM, Pan YP, Udan R, et al. Identification and characterization of small molecule inhibitors of the calcium-dependent S100B-p53 tumor suppressor interaction. J Med Chem 2004;47(21):5085–93 [English].

[11] Lee EJ, Khan SA, Park JK, Lim KH. Studies on the characteristics of drug-loaded gelatin nanoparticles prepared by nanoprecipitation. Bioprocess and biosystems engineering 2012;35(1–2):297–307 [eng].

[12] Rajan M, Raj V. Formation and characterization of chitosan-polylacticacid-polyethylene glycol-gelatin nanoparticles: a novel biosystem for controlled drug delivery. Carbohydr Polym 2013;98(1):951–8 [eng].

[13] Madan J, Pandey RS, Jain UK, Katare OP, Aneja R, Katyal A. Sterically stabilized gelatin microassemblies of noscapine enhance cytotoxicity, apoptosis and drug delivery in lung cancer cells. Colloids Surf B Biointerfaces 2013;107:235–44 [eng].

[14] Lee SJ, Yhee JY, Kim SH, Kwon IC, Kim K. Biocompatible gelatin nanoparticles for tumor-targeted delivery of polymerized siRNA in tumor-bearing mice. J Contr Release : official journal of the Controlled Release Society 2013;172(1):358–66 [eng].

[15] Wang J, Wu W, Zhang Y, Wang X, Qian H, Liu B, et al. The combined effects of size and surface chemistry on the accumulation of boronic acid-rich protein nanoparticles in tumors. Biomaterials 2014;35(2):866–78 [eng].

[16] Foox M, Zilberman M. Drug delivery from gelatin-based systems. Expet Opin Drug Deliv 2015;12(9):1547–63 [eng].

[17] Liu Q, Yu Y, Reisdorf RL, Qi J, Lu CK, Berglund LJ, et al. Engineered tendon-fibrocartilage-bone composite and bone marrow-derived mesenchymal stem cell sheet augmentation promotes rotator cuff healing in a non-weight-bearing canine model. Biomaterials 2019;192:189–98 [eng].

[18] Kadar A, Liu H, Vrieze AM, Meier TR, Thoreson AR, Amadio PC, et al. Establishment of an in vivo Turkey model for the study of flexor tendon repair. J Orthop Res 2018;36(9):2497–505 [eng].

[19] Heidari M, Bahrami SH, Ranjbar-Mohammadi M, Milan PB. Smart electrospun nanofibers containing PCL/gelatin/graphene oxide for application in nerve tissue engineering. Mater Sci Eng C 2019;103:109768.

[20] Ozasa Y, Amadio PC, Thoreson AR, An K-N, Zhao C. Repopulation of Intrasynovial flexor tendon Allograft with bone Marrow Stromal cells: AnEx VivoModel. Tissue engineering Part A. 2013, 131121072458005.

[21] Wu J, Thoreson AR, Reisdorf RL, An K-N, Moran SL, Amadio PC, et al. Biomechanical evaluation of flexor tendon graft with different repair techniques and graft surface modification. J Orthop Res 2015;33(5):731–7.

[22] Parks AN, McFaline-Figueroa J, Coogan A, Poe-Yamagata E, Guldberg RE, Platt MO, et al. Supraspinatus tendon overuse results in degenerative changes to tendon insertion region and adjacent humeral cartilage in a rat model. J Orthop Res : official publication of the Orthopaedic Research Society 2017;35(9):1910–8 [eng].

[23] Tanaka T, Sun YL, Zhao C, Zobitz ME, An KN, Amadio PC. Optimization of surface modifications of extrasynovial tendon to improve its gliding ability in a canine model in vitro. J Orthop Res : official publication of the Orthopaedic Research Society 2006;24(7):1555–61 [eng].

[24] Tanaka T, Sun YL, Zhao C, Zobitz ME, An KN, Amadio PC. Effect of curing time and concentration for a chemical treatment that improves surface gliding for extrasynovial tendon grafts in vitro. J Biomed Mater Res 2006;79(3):451–5 [eng].

[25] Zhao C, Amadio PC, Momose T, Couvreur P, Zobitz ME, An KN. Effect of synergistic wrist motion on adhesion formation after repair of partial flexor digitorum profundus tendon lacerations in a canine model in vivo. J Bone Joint Surg Am 2002;84(1):78–84 [eng].

[26] Zhao C, Sun Y-L, Ikeda J, Kirk RL, Thoreson AR, Moran SL, et al. Improvement of flexor tendon reconstruction with carbodiimide-derivatized hyaluronic acid and gelatin-modified intrasynovial Allografts. The Journal of Bone and Joint Surgery-American 2010;92(17):2817–28.

[27] Zhao C, Sun Y-L, Kirk RL, Thoreson AR, Jay GD, Moran SL, et al. Effects of a lubricin-containing compound on the results of flexor tendon repair in a canine model in vivo. The Journal of Bone and Joint Surgery-American 2010;92(6):1453–61.

[28] Zhao C, Amadio PC, Berglund L, Zobitz ME, An KN. A new testing device for measuring gliding resistance and work of flexion in a digit. J Biomech 2003;36(2):295–9 [eng].

[29] Uchiyama S, Coert JH, Berglund L, Amadio PC, An KN. Method for the measurement of friction between tendon and pulley. J Orthop Res : official publication of the Orthopaedic Research Society 1995;13(1):83–9 [eng].

[30] Zheng W, Chen C, Chen S, Fan C, Ruan H. Integrated analysis of long non-coding RNAs and mRNAs associated with peritendinous fibrosis. J Adv Res 2019;15:49–58 [eng].

[31] Armstrong D, Bernard E. Aerosol pentamidine. Ann Intern Med 1988;109(11):852–4 [eng].

[32] Goa KL, Campoli-Richards DM. Pentamidine isethionate. A review of its antiprotozoal activity, pharmacokinetic properties and therapeutic use in Pneumocystis carinii pneumonia. Drugs 1987;33(3):242–58 [eng].

[33] Zhao C. Surface treatment of flexor tendon Autografts with carbodiimide-derivatized hyaluronic Acid<sbt aid="1047845">An in vivo canine model</sbt&gt. J Bone Joint Surg 2006;88(10):2181.

[34] Schlag G, Redl H. Fibrin sealant in orthopedic surgery. Clin Orthop Relat Res 1988;227:269–85 [eng].

[35] Wei Z, Reisdorf RL, Thoreson AR, Jay GD, Moran SL, An K-N, et al. Comparison of Autograft and Allograft with surface modification for flexor tendon reconstruction. J Bone Joint Surg 2018;100(7):e42.

[36] Kwan KH, Yeung KW, Liu X, Wong KK, Shum HC, Lam YW, et al. Silver nanoparticles alter proteoglycan expression in the promotion of tendon repair. Nanomed Nanotechnol Biol Med 2014;10(7):1375–83 [eng].

[37] Zhou Y, Zhang L, Zhao W, Wu Y, Zhu C, Yang Y. Nanoparticle-mediated delivery of TGF-β1 miRNA plasmid for preventing flexor tendon adhesion formation. Biomaterials 2013;34(33):8269–78.

[38] Echave MC, Saenz del Burgo L, Pedraz JL, Orive G. Gelatin as biomaterial for tissue engineering. Curr Pharmaceut Des 2017;23(24):3567–84 [eng].

[39] Li LL, Xu JH, Qi GB, Zhao X, Yu F, Wang H. Core-shell supramolecular gelatin nanoparticles for adaptive and "on-demand" antibiotic delivery. ACS Nano 2014;8(5):4975–83 [eng].

[40] Klotz BJ, Gawlitta D, Rosenberg A, Malda J, Melchels FPW. Gelatin-methacryloyl hydrogels: towards Biofabrication-based tissue repair. Trends Biotechnol 2016;34(5):394–407 [eng].

[41] Liu D, Nikoo M, Boran G, Zhou P, Regenstein JM. Collagen and gelatin. Annu Rev Food Sci Technol 2015;6:527–57 [eng].

[42] Zhang Y, Sun T, Jiang C. Biomacromolecules as carriers in drug delivery and tissue engineering. Acta Pharm Sin B 2018;8(1):34–50 [eng].

[43] Ogawa Y, Azuma K, Izawa H, Morimoto M, Ochi K, Osaki T, et al. Preparation and biocompatibility of a chitin nanofiber/gelatin composite film. Int J Biol Macromol 2017;104(Pt B):1882–9 [eng].

[44] Zhang M, Zhen J, Zhang X, Yang Z, Zhang L, Hao D, et al. Effect of Autologous platelet-rich plasma and gelatin sponge for tendon-to-bone healing after rabbit anterior cruciate Ligament reconstruction. Arthroscopy : the journal of arthroscopic & related surgery : official publication of the Arthroscopy Association of North America and the International Arthroscopy Association 2019;35(5):1486–97 [eng].

[45] Bhavsar D, Shettko D, Tenenhaus M. Encircling the tendon repair site with collagen-GAG reduces the formation of postoperative tendon adhesions in a chicken flexor tendon model. J Surg Res 2010;159(2):765–71 [eng].

[46] Zhao T, Qi Y, Xiao S, Ran J, Wang J, Ghamor-Amegavi EP, et al. Integration of mesenchymal stem cell sheet and bFGF-loaded fibrin gel in knitted PLGA scaffolds favorable for tendon repair. J Mater Chem B 2019;7(13):2201–11 [eng].

[47] Chong AKS, Riboh J, Smith RL, Lindsey DP, Pham HM, Chang J. Flexor tendon tissue engineering: acellularized and reseeded tendon constructs. Plast Reconstr Surg 2009;123(6):1759–66 [eng].

[48] Li X, Chen H, Xie S, Wang N, Wu S, Duan Y. Fabrication of Photo-Crosslinkable Poly(Trimethylene Carbonate)/Polycaprolactone Nanofibrous Scaffolds for Tendon Regeneration 2020;15:6373–83.

[49] Yamamoto-Shiraishi Y, Kuroiwa A. Wnt and BMP signaling cooperate with Hox in the control of Six2 expression in limb tendon precursor. Dev Biol 2013;377(2):363–74 [eng].

[50] Lorda-Diez CI, Montero JA. Four and a half domain 2 (FHL2) scaffolding protein is a marker of connective tissues of developing digits and regulates fibrogenic differentiation of limb mesodermal progenitors 2018;12(4):e2062–72.

[51] Vallon M, Yuki K, Nguyen TD, Chang J, Yuan J, Siepe D, et al. A RECK-WNT7 Receptor-Ligand interaction enables isoform-specific regulation of Wnt Bioavailability. Cell Rep 2018;25(2):339–49. e9. [eng].

[52] Andre P, Song H, Kim W, Kispert A, Yang Y. Wnt5a and Wnt11 regulate mammalian anterior-posterior axis elongation. Development 2015;142(8):1516–27.

[53] Yoshioka S, King ML, Ran S, Okuda H, MacLean 2nd JA, McAsey ME, et al. WNT7A regulates tumor growth and progression in ovarian cancer through the WNT/β-catenin pathway. Mol Cancer Res : MCR 2012;10(3):469–82 [eng].

[54] Kraft B, Berger CD, Wallkamm V, Steinbeisser H, Wedlich D. Wnt-11 and Fz7 reduce cell adhesion in convergent extension by sequestration of PAPC and C-cadherin. JCB (J Cell Biol) 2012;198(4):695–709.

[55] Puech PH, Taubenberger A, Ulrich F, Krieg M, Muller DJ, Heisenberg CP. Measuring cell adhesion forces of primary gastrulating cells from zebrafish using atomic force microscopy. J Cell Sci 2005;118(Pt 18):4199–206 [eng].

[56] Oteiza P, Köppen M, Krieg M, Pulgar E, Farias C, Melo C, et al. Planar cell polarity signalling regulates cell adhesion properties in progenitors of the zebrafish laterality organ. Development 2010;137(20):3459–68 [eng].

[57] Iizumi R, Honda M. Wnt/β-Catenin signaling inhibits Osteogenic differentiation in human Periodontal Ligament fibroblasts. Biomimetics 2022;7(4) [eng].
[58] Kishimoto Y, Ohkawara B, Sakai T, Ito M, Masuda A, Ishiguro N, et al. Wnt/β-catenin signaling suppresses expressions of Scx, Mkx, and Tnmd in tendon-derived cells. PLoS One 2017;12(7):e0182051 [eng].
[59] Lui PP, Lee YW, Wong YM, Zhang X, Dai K, Rolf CG. Expression of Wnt pathway mediators in metaplasic tissue in animal model and clinical samples of tendinopathy. Rheumatology 2013;52(9):1609–18 [eng].
[60] Wang Y, Tang H, He G, Shi Y, Kang X, Lyu J, et al. High concentration of Aspirin induces apoptosis in rat tendon stem cells via inhibition of the Wnt/β-catenin pathway. Cell Physiol Biochem 2018;50(6):2046–59 [eng].
[61] Deshmukh V, Seo T, O'Green AL, Ibanez M, Hofilena B, Kc S, et al. SM04755, a small-molecule inhibitor of the Wnt pathway, as a potential topical treatment for tendinopathy. J Orthop Res 2021;39(9):2048–61 [eng].